Fatal infantile cardioencephalomyopathy with COX deficiency and mutations in *SCO2*, a COX assembly gene

Lefkothea C. Papadopoulou[1], Carolyn M. Sue[2], Mercy M. Davidson[2], Kurenai Tanji[2], Ichizo Nishino[2], James E. Sadlock[2], Sindu Krishna[2], Winsome Walker[2], Jeanette Selby[3], D. Moira Glerum[6], Rudy Van Coster[7], Gilles Lyon[7], Emmanuel Scalais[8], Roger Lebel[9], Paige Kaplan[10], Sara Shanske[2], Darryl C. De Vivo[2], Eduardo Bonilla[2,4], Michio Hirano[2], Salvatore DiMauro[2] & Eric A. Schon[2,5]

Mammalian cytochrome *c* oxidase (COX) catalyses the transfer of reducing equivalents from cytochrome *c* to molecular oxygen and pumps protons across the inner mitochondrial membrane[1]. Mitochondrial DNA (mtDNA) encodes three COX subunits (I–III) and nuclear DNA (nDNA) encodes ten. In addition, ancillary proteins are required for the correct assembly and function of COX (refs 2–6). Although pathogenic mutations in mtDNA-encoded COX subunits have been described[7], no mutations in the nDNA-encoded subunits have been uncovered in any mendelian-inherited COX deficiency disorder[8–13]. In yeast, two related COX assembly genes, *SCO1* and *SCO2* (for synthesis of cytochrome *c* oxidase), enable subunits I and II to be incorporated into the holoprotein. Here we have identified mutations in the human homologue, *SCO2*, in three unrelated infants with a newly recognized fatal cardioencephalomyopathy and COX deficiency. Immunohistochemical studies implied that the enzymatic deficiency, which was most severe in cardiac and skeletal muscle, was due to the loss of mtDNA-encoded COX subunits. The clinical phenotype caused by mutations in human *SCO2* differs from that caused by mutations in *SURF1*, the only other known COX assembly gene associated with a human disease, Leigh syndrome[14,15].

Two human loci encode SCO-like proteins: *SCO1* (ref. 4), located on chromosome 17p12–13, and *SCO2*, located on chromosome 22q13. Human *SCO2* contains two exons (nt 1–63 and 1,111–1,965) and one intron (nt 64–1,110). Exon 1 encodes part of the 5′ UTR; exon 2 contains the remaining 13 bp of the 5′ UTR, an 801-bp coding region and a 41-bp 3′ UTR containing a polyadenylation signal (ATTAAA), for a total length of 918 nt.

The deduced human SCO2 protein (266 aa; Fig. 1) predicts an amino-terminal mitochondrial targeting presequence (41 aa; cleavage between Gln-41 and Gly-42). Alignment of human and yeast SCO polypeptides (Fig. 1) shows that they share the greatest identity in a 'core' region between Gly-102 and Gly-242 of human SCO2, including Cys-133, Cys-137 and His-224. In this region, the amino acid identity between the two human proteins (54%) is less than that between the two yeast proteins (73%). Moreover, human SCO2 and SCO1 show similar divergence from both yeast proteins (SCO2, 43% and 40% for Sco1p and Sco2p, respectively; SCO1, 39% and 41%, respectively). Thus, it appears

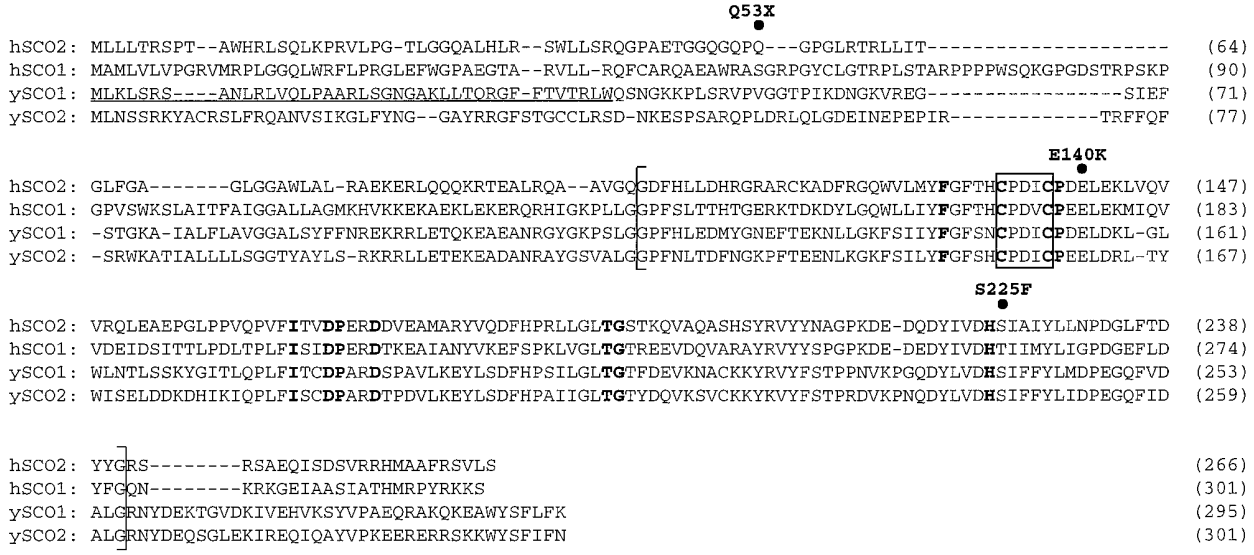

Fig. 1 Alignment of the deduced yeast (y) and human (h) SCO polypeptides (sizes, in amino acids, at right). The presequence of yeast SCO1 (A. Tzagoloff, pers. comm.) is underlined. The 'core' region of greatest sequence identity is flanked by brackets. The amino acids in bold are those conserved among the SCO and SCO-like polypeptides found in a search of GenBank. The CXXXC motif is boxed. The three pathogenic point mutations are indicated by dots.

[1]*Department of Pharmaceutical Sciences, Aristotle University of Thessaloniki, Thessaloniki, Macedonia, Greece. Departments of* [2]*Neurology,* [3]*Pediatrics,* [4]*Pathology, and* [5]*Genetics and Development, Columbia University, New York, New York, USA.* [6]*Department of Medical Genetics, University of Alberta, Edmonton, Canada.* [7]*Kinderkliniek "C. Hoopt," University Hospital, Ghent, Belgium.* [8]*Clinique St. Vincent, Liege, Belgium.* [9]*Genetics Services, Inc., Glen Ellyn, Illinois, USA.* [10]*Division of Metabolism, Children's Hospital of Philadelphia, Philadelphia, Pennsylvania, USA. Correspondence should be addressed to E.A.S. (e-mail: eas3@columbia.edu).*

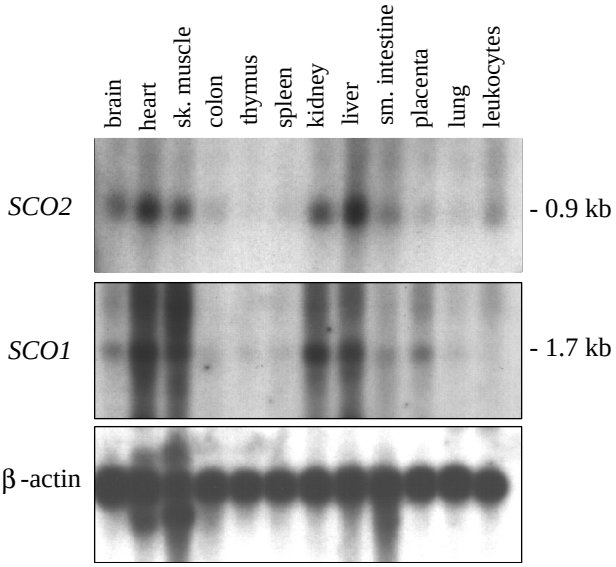

Fig. 2 Northern-blot hybridization of human mRNA from the indicated tissues with probes specific for *SCO1*, *SCO2* and β-actin.

that the two human genes are not orthologous to the two yeast genes (that is, they did not diverge from a common ancestral gene pair), but rather are paralogous genes (that is, gene duplication occurred independently in the two lineages).

In northern-blot analysis, a *SCO2* coding-region probe hybridized to a 0.9-kb transcript in all 12 human tissues examined (Fig. 2). The strongest signals were present in heart, skeletal muscle, brain, liver and kidney. A probe derived from the 3′ UTR of *SCO1* hybridized to a 1.7-kb transcript[4] in the same 12 tissues (Fig. 2). As with *SCO2*, the strongest signals were in heart, skeletal muscle, brain, liver and kidney, but comparison of the blot intensities suggested that the steady-state level of *SCO1* transcripts in these tissues was greater than that of *SCO2* transcripts.

We identified mutations in *SCO2* in three patients with COX deficiency; all presented with a fatal infantile cardioencephalomyopathy. None of the patients had a family history of neuromuscular disease. Heart and skeletal muscle showed reductions in COX activity, whereas liver and fibroblasts had mild COX deficiencies (Table 1). Histochemistry of muscle from patients 2 and 3 showed reductions in COX enzyme activity in all fibres (Fig. 3*d–f*), but succinate dehydrogenase (SDH) activity appeared normal (Fig. 3*a–c*); there were no ragged-red fibres. Immunohistochemistry showed a severe reduction of the mtDNA-encoded COX I (Fig. 3*j–l*) and II (Fig. 3*m–o*) subunits, whereas the nDNA-encoded COX subunits IV (Fig. 3*p–r*) and Va (data not shown) were present but reduced in intensity. The nDNA-encoded Rieske iron-sulphur subunit of complex III appeared normal in both patients (Fig. 3*g–i*).

Patients 1 and 3 carried two identical mutations in *SCO2* (Fig. 4): a C→T transition at nt 1,280 creating a stop codon at Gln-53 (Q53X), and a G→A transition at nt 1,541 converting Glu-140 to Lys (E140K). Patient 2 was also a compound heterozygote: she carried the same G1541A (E140K) mutation found in patients 1 and 3, plus a C→T transition at nt 1,797 converting Ser-225 to Phe (S225F; Fig. 4). Each of the six parents was heterozygous for a single mutation (data not shown).

We believe that the mutations in *SCO2* in the three infants with fatal cardioencephalomyopathy are aetiologic. First, human *SCO2* is a homologue of yeast *SCO1* and *SCO2*. Sco1p is required for the assembly of subunits I and II into the holoprotein, and, like Cox17p, is required for the transport of copper to COX (refs 16–21). Overexpression of *SCO1* can rescue respiratory-deficient yeast cells harbouring either a *COX17* null mutation or a *COX17* point mutation[20]. The function of Sco2p is less clear, as yeast *SCO2* mutants do not show respiratory deficiency, and overexpression of *SCO2* rescued only the *COX17* point mutation, not the null mutation[20]. Second, the Q53X nonsense mutation, found in two of three patients, truncates the protein upstream of the putative functionally conserved 'core' region of SCO2.

Third, all known SCO proteins contain a conserved pair of cysteines, separated by three residues, that have been proposed to bind copper, similar to the CXXXC motif in COX II (ref. 20) that binds two copper atoms (subunit I binds a third Cu, via His residues[1]). The E140K mutation, found in all three patients, is adjacent to the postulated SCO2 CXXXC copper-binding motif between Cys-133 and Cys-137; these two residues are essential for function in yeast Sco1p (ref. 22). Moreover, this mutation converts a highly conserved, negatively charged glutamate to a positively charged lysine (aa 140 is either Glu or Asp in 13 of 18 aligned polypeptides, but is never a basic residue). A positively charged residue would likely displace, rather than stabilize, copper in the Cu-binding domain. Similarly, the S225F mutation, located next to the highly conserved His-224, converts an uncharged polar moiety (Ser or Thr in 16/18 aligned polypeptides) to a hydrophobic residue that may also interfere with the function of SCO2. Thus, if human SCO2 were required for the insertion of copper into the COX holoprotein, subunits I and II would be primarily affected by loss-of-function mutations in *SCO2*. The immunohistochemistry results (Fig. 3) are consistent with this idea, but we note that Cox1p and Cox2p may also be lost in yeast assembly mutants that are not associated with copper transport[23].

Fourth, the pattern of *SCO2* transcription is consistent with the clinical presentation of cardioencephalomyopathy, in that heart, brain and skeletal muscle have high amounts of *SCO2* mRNA, and in that we observed reductions of COX activity in heart and skeletal muscle (Table 1). Although liver also expresses high levels of *SCO2* mRNA and was clinically affected in two patients, COX deficiency was less severe in this tissue[24]. In addition, patients presenting with early and severe cardiomyopathy and COX deficiency in heart have had normal COX activity in liver, fibroblasts or both[24]. Conversely, some patients with encephalopathy and hepatopathy have more severe COX activities in brain and liver than in muscle or heart[25].

Although *SCO1* and *SCO2* transcription appears ubiquitous, it may be that the corresponding polypeptides are not present in all tissues[26,27]. In fact, the two SCO isoforms do not appear to be functionally equivalent in yeast, as the *SCO1* null was not com-

Table 1 • COX activity in patient tissues

		Patient		
	Controls	1	2	3
Skeletal muscle[a]	0.28±0.05 (n=69)	0.01 (4%)	0.01 (4%)	0.05 (18%)
Heart[a]	0.13±0.04 (n=10)	0.01 (8%)	NA	0.01 (8%)
Liver[a]	0.25±0.08 (n=17)	0.04 (16%)	NA	0.13 (52%)
Fibroblasts[b]	0.73±0.30 (n=13)	0.09 (12%)	NA	0.22 (30%)

Activity normalized to that of citrate synthase in [a]μmoles/min/g protein or [b]μmoles/min/ml homogenate. Control values are±s.d.; n, number of controls; % of control activity is in parentheses; NA, tissue not available.

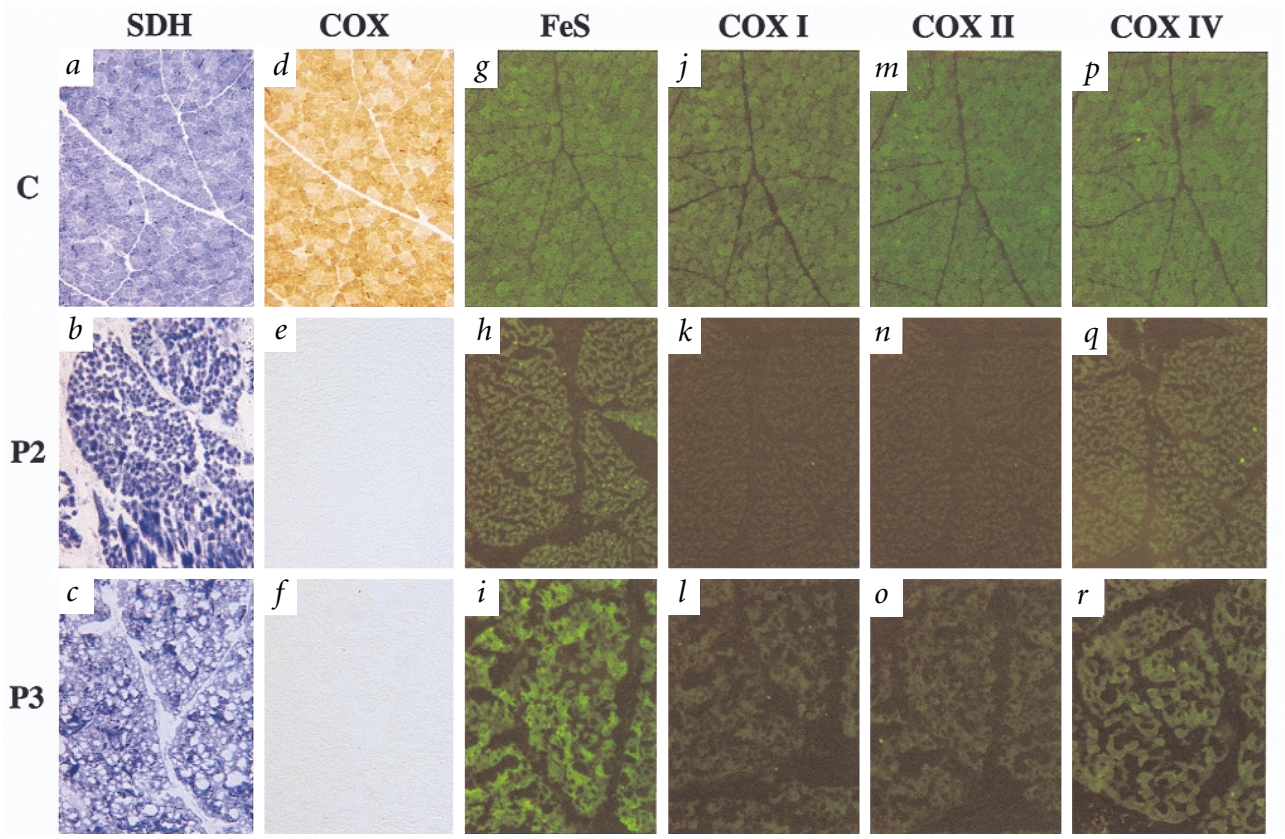

Fig. 3 Morphology of muscle serial sections from patients 2 (P2) and 3 (P3) compared with control (C). Histochemical staining to detect succinate dehydrogenase (SDH; ***a***,***b***,***c***) and cytochrome *c* oxidase (COX; ***d***,***e***,***f***) enzyme activities are shown, as well as immunohistochemical staining to detect COX subunits I (***j***,***k***,***l***), II (***m***,***n***,***o***) and IV (***p***,***q***,***r***), and the Rieske iron-sulphur protein (FeS) subunit of complex III (***g***,***h***,***i***).

plemented by overexpression of yeast or human *SCO2* cDNAs (ref. 28, and data not shown). More work is needed to establish the role of SCO2 in COX assembly and function and the mechanisms by which mutations in *SCO2* cause disease.

Methods

Patients. Patient 1 (T.B.) was a 3,950-g product of a full-term uneventful pregnancy. He developed inspiratory stridor, irregular respirations, exotropia and nystagmus. At 6 weeks he was found unresponsive and in cardiopulmonary shock, and was placed on a ventilator. Echocardiogram revealed a hypertrophic cardiomyopathy. The infant never regained consciousness. Cranial nerves, including the fundus, were normal. He had severe hypotonia and occasional limb dystonia. Tendon reflexes were present; plantar responses were absent. Arterial lactate was increased (9.8 mM; normal <2.2 mM) with an elevated lactate/pyruvate ratio (36, normal <20). Cerebrospinal fluid (CSF) lactate was also elevated (3.9 mM; normal <2 mM). Brainstem auditory evoked responses and somatosensory evoked potentials revealed increased central conduction times. At 11 weeks he had a cardiac arrest and died. At autopsy, the liver was enlarged (240 g) but the brain was grossly normal. Microscopically, gliosis and microglial cell proliferation were seen in the lateral globus pallidus, putamen and ventroposterolateral (VPL) thalamus. Moderate neuronal loss with some chromatolytic neurons and neuronophagic nodules were seen in the VPL thalamus. The medulla showed bilateral spongiform necrosis in the ventral aspect of the olives. The distribution of the gliosis, relative neuronal preservation and bilateral necrotic lesions in the medulla was more compatible with Leigh syndrome than with ischaemic injury.

Patient 2 (E.H.) was a 2,910-g product of a normal pregnancy and delivery. At 10 weeks she suffered a cardiopulmonary arrest and was intubated. Echocardiogram revealed a hypertrophic cardiomyopathy. The infant remained on a ventilator. Examination revealed dysmorphic features: dolichocephaly with a depressed nasal bridge, a high-arched palate, hypoplastic toenails of the fourth and fifth digits, and anteriorly displaced finger-like thumbs. Electroencephalogram revealed rare, focal epileptiform discharges in both central temporal areas. At 3 months, electromyography (EMG) was consistent with a myopathy. At 4 months, nerve conduction studies revealed a mixed axonal and demyelinating sensorimotor neuropathy. Venous lactate was 3.3 mM (normal 0.5–2.2 mM) and venous pyruvate was 1.4 mM (normal 0.3–0.9 mM). At 5 months, computed tomography (CT) scan showed cerebral atrophy with enlarged ventricles and prominent sulci. At 6 months, CT revealed more prominent brain atrophy. The child died at 6 months. On autopsy, hepatomegaly was prominent without splenomegaly, ascites or peripheral edema. The brain was atrophic (470 g). There was bilateral necrosis of the globus pallidus. Sommer sector of the hippocampi, cerebral white matter, thalami, brainstem and cerebellar nuclei were atrophied. There was atrophy of the deep and lateral cerebellar hemispheres within watershed territories. The spinal cord showed atrophy of the descending tracts, diffuse gliosis and moderate patchy loss of motor neurons.

Patient 3 (M.C.) was a full-term 3,460-g product of a normal pregnancy and delivery. She was mildly hypotonic after birth. At 15 h, a cardiac murmur was detected. Echocardiogram revealed mild septal hypertrophy. She developed increasing lethargy and difficulty in feeding and breathing. At 1 month she was admitted with respiratory distress, poor perfusion and diaphoresis. Venous lactate was elevated at 2.7 mM (normal 0.8–2.0 mM) with a borderline pyruvate level of 0.14 mM (normal 0.05–0.14 mM). CSF lactate was also elevated at 3.4 mM (normal 0.7–2.0 mM), CSF pyruvate was normal and CSF lactate/pyruvate ratio was elevated at 38 (normal 10–20). She was placed on a ventilator. A second echocardiogram revealed a severely thickened left ventricle with no evidence of outflow obstruction. At 37 d, the liver was palpable 2 cm below the costal margin. A brain magnetic resonance image (MRI) was normal. At 42 d, a third echocardiogram revealed more severe cardiac hypertrophy and obliteration of the left ventricular cavity during systole. After ventilatory support was withdrawn, the patient died at 53 d. Autopsy revealed a grossly enlarged globular heart

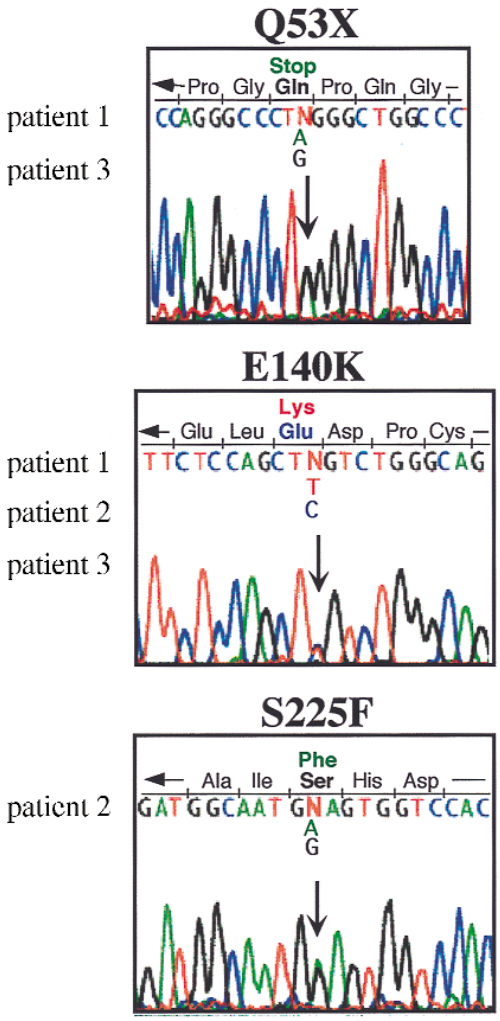

Fig. 4 Detection of *SCO2* mutations in cardioencephalomyopathy patients. Representative electropherograms of the DNA (antisense strand) and deduced amino acid sequences in the region of each mutation (arrows) in the indicated patients are shown.

(115 g), a mildly enlarged liver (160 g) and brain atrophy (424 g). The cardiac left ventricle and septum were grossly hypertrophic. The liver was congested. The cerebral hemisphere showed an abnormal gyral pattern. The left hemisphere gyri of the frontal, temporal and parietal opercula radiated toward the Sylvian fissure. The left temporal lobe had rudimentary superior and middle temporal gyri. The right hemisphere had umbilicated gyri centred on the posterior right Sylvian fissure. Cerebral cortex, white matter, basal ganglia, thalami and ventricles were normal. Microscopic examination of the heart revealed myocardial fibre disarray and occasional myocyte hypertrophy. Many cardiomyocytes, especially in the septum, had a 'moth-eaten' appearance with rims of darkly staining cytoplasm surrounding clear centers. Skeletal muscle showed rounded myocytes with increased variation of fibre size. Brain histology showed cerebral white matter gliosis with focal white matter necrosis and petechial haemorrhages, focal cortical dysplasia of the left temporal lobe and mild cortical and hippocampal neuronal dropout. The cerebellum had a focal heterotopia and collections of granular cell neurons in the dentate nucleus. A chronic inflammatory leptomeningeal infiltrate was noted and was more prominent over the spinal cord. The spinal cord showed mild gliosis and white matter spongiosis.

Biochemistry. We performed respiratory chain activities on biopsy and autopsy samples as described[24].

Morphology. We used frozen muscle sections (8 μm) from patients 2 and 3 and from a normal control for COX and SDH histochemistry, and additional sections (4 μm) for immunohistochemical studies, as described[29].

Isolation of human *SCO2* sequences. We screened a library of human T-cell cDNA inserted into LambdaZap Express (Stratagene), with a human *SCO2* coding-region probe. We PCR amplified the probe from genomic DNA with forward primer F3 (nt 1,520–1,546) and backward primer B3 (nt 1,801–1,774), labelled with [α-^{32}P]dATP by random priming to a specific activity of 5×10^8 cpm/μg, hybridized overnight at 55 °C, washed at 55 °C and autoradiographed using Kodak XAR-5 film at –70 °C with an intensifying screen. Ten positive plaques were picked and purified, and were converted first to pBK-CMV phagemids and then to the corresponding pBK-CMV plasmids, according to the manufacturer's protocol. We sequenced plasmid inserts with the fmol DNA sequencing kit (Promega) using vector primers as well as *SCO2*-specific primers F1 (nt 1,124–1,156), F3, F4 (nt 1,899–1,920), B1 (nt 1,924–1,899) and B4 (nt 1,232–1,214). The insert of one clone, pHSCO1.10.2, appeared full-length, and it allowed us to identify the exon/intron boundaries of the gene. We used primers F5 (nt 1–23) and either B5 (nt 1,960–1,940) or B6 (nt 1,999–1,979) to amplify the gene. The genomic sequence of human *SCO2* has been submitted to GenBank; the map coordinates noted in the text are based on the numbering of this sequence.

Analysis of polypeptides. We predicted the cleavage site for the SCO2 presequence using the MitoProt algorithm (http://websvr.mips.biochem.mpg.de/cgi-bin/proj/medgen/mitofilter). We aligned human and yeast SCO polypeptide sequences with the following SCO and SCO-like sequences: *Anaplasma marginale* msp5; *Aquifex aeolicus*; *Bacillus* sp. mnxC; *Bacillus subtilis* ypmQ; *Caenorhabditis elegans* SCO1; *Cowdria ruminantium*; *Homo sapiens* SCO1; *Homo sapiens* SCO2; *Plasmodium falciparum* CG3; *Pseudomonas stutzeri* ORF-193; *Rhodobacter spheroides* prrC; *Rhodobacter spheroides* regC; *Rhodovulum sulfidophilum* senC; *Rickettsia prowazekii* SCO2-2; *Rosebacter denitrificans* senC; *Saccharomyces cerevisiae* SCO1; *Saccharomyces cerevisiae* SCO2; and *Schizosaccharomyces pombe* SCO1.

Northern-blot hybridization analysis. We used the human 12-lane multiple-tissue northern (MTN) blot (Clontech). Radiolabelled probes were made using the Random Primed DNA labelling kit (Boehringer) with [α-^{32}P]dATP. We carried out hybridization according to the manufacturer's protocol, and autoradiographed on Kodak XAR-5 film at –70 °C with an intensifying screen. The membrane was stripped of the hybridized probe by immersion in boiling 0.5% SDS for 10 min, and re-exposed to confirm removal of the probe before rehybridization. Sequential probes were as follows: *SCO2* (nt 1,124–1,960), exposed for 17 d; *SCO1* (nt 958–1,512), exposed for 3 d; and a human β-actin probe, exposed for 15 h. Each SCO probe also detected a much larger unknown transcript (~4 kb for *SCO2* and 5 kb for *SCO1*; data not shown).

Screening for mutations in human *SCO2*. We amplified full-length *SCO2* from patient total DNA with primers F5 and B5 with an initial cycle of 94 °C for 2 min, 30 cycles of 94 °C for 1 min, 60 °C for 2 min and 72 °C for 3 min, followed by a last cycle of extension at 72 °C for 10 min. PCR reactions contained 10% DMSO to facilitate extension through regions of secondary structure. PCR products were purified from agarose (QIAquick gel extraction kit, Qiagen), re-amplified and re-extracted, and sequenced using the ABI PRISM Dye Terminator Cycle Sequencing Ready Reaction kit (Perkin Elmer) with primers F3, F5, F6 (nt 1,081–1,102), B3, B4, B5, B7 (nt 721–701) and B8 (nt 1,405–1,386). We confirmed mutations in at least two independent PCR amplification products from each patient. The Q53X, E140K and S225F mutations were absent in 60 normal controls and in 28 COX-deficient LS patients. We found a number of other mutations that were deemed to be neutral polymorphisms, as they were also in controls. These included point mutations in exon 1 (G59A), intron 1 (G310T, C424G) and exon 2 (G1182C, R20P), as well as a 15-bp deletion (removing nt 622–636) in intron 1. We also found two silent mutations in exon 2 (C1705T, S194S; A1756C, A211A).

RFLP analysis. For the Q53X nonsense mutation (C1280T), which destroys a *Bst*XI site and creates a new *Avr*II site, we amplified genomic

DNA with primers F5 and B5 (in some cases we amplified this PCR product with F1 and B1), and digested the resulting fragment with either *Bst*XI (Boerhinger) or *Avr*II (New England Biolabs). For the E140K missense mutation (G1541A), we performed nested PCR, first with primers F5 and B5 and then with primers F9 (nt 1,366–1,385) and a mismatched backward primer, B9 (nt 1,568–1,543; C→A at nt 1,546), designed to create a *Hin*dIII site in the mutated allele only. For the S225F missense mutation (C1797T), we performed nested PCR, first with primers F5 and B5, and then with mismatched primer F10 (nt 1,771–1,796; AA→GG at nt 1,789–1,790), designed to create a *Xmn*I site in the mutated allele only, and B1.

GenBank accession numbers. Human *SCO2*, AF177385; human *SCO1*, AF026852; *A. marginale* msp5, g477569; *A. aeolicus*, AE000717; *Bacillus* sp. mnxC, U31081; *B. subtilis* ypmQ, L77246; *C. elegans* SCO1, U58761; *C. ruminantium*, PID g2126378; *P. falciparum* CG3, AF030694; *P. stutzeri* ORF-193, Z26044; *R. spheroides* prrC, pir 2126490; *R. spheroides* regC, PID g746421; *R. sulfidophilum* senC, AB010722; *R. prowazekii* SCO2-2, AJ235272; *R. denitrificans* senC, AB010723; *S. cerevisiae* SCO1, X17441; *S. cerevisiae* SCO2, Z35893; *S. pombe* SCO1, AL022117.

Acknowledgements

We thank F. Guo, P. Kranz-Eberle, F. Pallotti, P. Magalhães, G. Manfredi, R. Pons and S. Tadesse for technical assistance; E. Holme, M. Huttermann, B. Kadenbach and M. Tulinius for patient samples; and A. Tzagoloff for communicating unpublished data. This work was supported by grants from the National Institutes of Health (NS28828, NS32527, NS11766, HL59657 and HD32062), the Muscular Dystrophy Association and a Neil Hamilton Fairley NHMRC Postdoctoral Fellowship (C.M.S.).

Received 22 April; accepted 17 August 1999.

1. Michel, H., Behr, J., Harrenga, A. & Kannt, A. Cytochrome *c* oxidase: structure and spectroscopy. *Annu. Rev. Biophys. Biomol. Struct.* **27**, 329–356 (1998).
2. Pel, H.J., Tzagoloff, A. & Grivell, L.A. The identification of 18 nuclear genes required for the expression of the yeast mitochondrial gene encoding cytochrome *c* oxidase subunit 1. *Curr. Genet.* **21**, 139–146 (1992).
3. Glerum, D.M. & Tzagoloff, A. Isolation of a human cDNA for heme A:farnesyltransferase by functional complementation of a yeast *cox10* mutant. *Proc. Natl Acad. Sci. USA* **91**, 8452–8456 (1994).
4. Petruzzella, V. *et al.* Identification and characterization of human cDNAs specific to *BCS1*, *PET112*, *SCO1*, *COX15*, and *COX11*, five genes involved in the formation and function of the mitochondrial respiratory chain. *Genomics* **15**, 494–504 (1998).
5. Amaravadi, R., Glerum, D.M. & Tzagoloff, A. Isolation of a cDNA encoding the human homolog of *COX17*, a yeast gene essential for mitochondrial copper recruitment. *Hum. Genet.* **99**, 329–333 (1997).
6. Bonnefoy, N. *et al.* Cloning of a human gene involved in cytochrome oxidase assembly by functional complementation of an *oxa1*$^{-}$ mutation in *Saccharomyces cerevisiae*. *Proc. Natl Acad. Sci. USA* **91**, 11978–11982 (1994).
7. Schon, E.A., Bonilla, E. & DiMauro, S. Mitochondrial DNA mutations and pathogenesis. *J. Bioenerg. Biomembr.* **29**, 131–149 (1997).
8. DiMauro, S. *et al.* Fatal infantile mitochondrial myopathy and renal dysfunction due to cytochrome-c-oxidase deficiency. *Neurology* **30**, 795–804 (1980).
9. DiMauro, S. *et al.* Benign infantile mitochondrial myopathy due to reversible cytochrome *c* oxidase deficiency. *Ann. Neurol.* **14**, 226–234 (1983).
10. Lombes, A. *et al.* Biochemical and molecular analysis of cytochrome *c* oxidase deficiency in Leigh's syndrome. *Neurology* **41**, 491–498 (1991).
11. DiMauro, S., Hirano, M., Bonilla, E., Moraes, C.T. & Schon, E.A. Cytochrome oxidase deficiency: progress and problems. in *Mitochondrial Disorders in Neurology* (eds Schapira, A.H.V. & DiMauro, S.) 91–115 (Butterworth-Heinemann, Oxford, 1994).
12. Adams, P.L., Lightowlers, R.N. & Turnbull, D.M. Molecular analysis of cytochrome *c* oxidase deficiency in Leigh's syndrome. *Ann. Neurol.* **41**, 268–270 (1997).
13. Jaksch, M. *et al.* A systematic mutation screen of 10 nuclear and 25 mitochondrial candidate genes in 21 patients with cytochrome *c* oxidase (COX) deficiency shows tRNA$^{(Ser)(UCN)}$ mutations in a subgroup with syndromal encephalopathy. *J. Med. Genet.* **35**, 895–900 (1998).
14. Zhu, Z. *et al. SURF1*, encoding a factor involved in the biogenesis of cytochrome *c* oxidase, is mutated in Leigh syndrome. *Nature Genet.* **20**, 337–343 (1998).
15. Tiranti, V. *et al.* Mutations of *SURF-1* in Leigh disease associated with cytochrome c oxidase deficiency. *Am. J. Hum. Genet.* **63**, 1609–1621 (1998).
16. Buchwald, P., Krummeck, G. & Rödel, G. Immunological identification of yeast SCO1 protein as a component of the inner mitochondrial membrane. *Mol. Gen. Genet.* **229**, 413–420 (1991).
17. Schulze, M. & Rödel, G. SCO1, a yeast nuclear gene essential for accumulation of mitochondrial cytochrome *c* oxidase subunit II. *Mol. Gen. Genet.* **211**, 492–498 (1988).
18. Schulze, M. & Rödel, G. Accumulation of the cytochrome *c* oxidase subunits I and II in yeast requires a mitochondrial membrane-associated protein, encoded by the nuclear *SCO1* gene. *Mol. Gen. Genet.* **216**, 37–43 (1989).
19. Krummeck, G. & Rödel, G. Yeast SCO1 protein is required for a post-translational step in the accumulation of mitochondrial cytochrome c oxidase subunits I and II. *Curr. Genet.* **18**, 13–15 (1990).
20. Glerum, D.M., Shtanko, A. & Tzagoloff, A. *SCO1* and *SCO2* act as high copy suppressors of a mitochondrial copper recruitment defect in *Saccharomyces cerevisiae*. *J. Biol. Chem.* **271**, 20531–20535 (1996).
21. Glerum, D.M., Shtanko, A. & Tzagoloff, A. Characterization of *COX17*, a yeast gene involved in copper metabolism and assembly of cytochrome oxidase. *J. Biol. Chem.* **271**, 14504–14509 (1996).
22. Rentzsch, A. *et al.* Mitochondrial copper metabolism in yeast: mutational analysis of Sco1p involved in the biogenesis of cytochrome *c* oxidase. *Curr. Genet.* **35**, 103–108 (1999).
23. McEwen, J.E., Ko, C., Kloeckner-Gruissem, B. & Poyton, R.O. Nuclear functions required for cytochrome *c* oxidase biogenesis in *Saccharomyces cerevisiae*. *J. Biol. Chem.* **261**, 11872–11879 (1986).
24. DiMauro, S. *et al.* Cytochrome *c* oxidase deficiency in Leigh syndrome. *Ann. Neurol.* **22**, 498–506 (1987).
25. Merante, F. *et al.* A biochemically distinct form of cytochrome oxidase (COX) deficiency in the Saguenay-Lac-Saint-Jean region of Quebec. *Am. J. Hum. Genet.* **53**, 481–487 (1993).
26. Taanman, J.-W., Herzberg, N.H., De Vries, H., Bolhuis, P.A. & Van den Bogert, C. Steady-state transcript levels of cytochrome c oxidase genes during human myogenesis indicate subunit switching of subunit VIa and co-expression of subunit VIIa isoforms. *Biochim. Biophys. Acta* **1139**, 155–162 (1992).
27. Preiss, T. & Lightowlers, R.N. Post-transcriptional regulation of tissue-specific isoforms. A bovine cytosolic RNA-binding protein, COLBP, associates with messenger RNA encoding the liver-form isopeptides of cytochrome *c* oxidase. *J. Biol. Chem.* **268**, 10659–10667 (1993).
28. Paret, C., Ostermann, K., Krause-Buchholz, U., Rentzsch, A. & Rödel, G. Human members of the SCO1 gene family: complementation analysis in yeast and intracellular localization. *FEBS Lett.* **447**, 65–70 (1999).
29. Sciacco, M. & Bonilla, E. Cytochemistry and immunocytochemistry of mitochondria in tissue sections. *Methods Enzymol.* **264**, 509–521 (1996).